Acc. Chem. Res. **1999,** *32,* 783−793

Intrazeolite Photochemistry: Toward Supramolecular Control of Molecular Photochemistry

J. C. SCAIANO*,† AND
HERMENEGILDO GARCÍA*,‡

Department of Chemistry, University of Ottawa, Ottawa K1N 6N5, Canada, and Instituto Tecnología Química, Apartado 22012, 46071 Valencia, Spain

Received September 14, 1998

Introduction

Selectivity in ground-state reactions is commonly achieved by developing appropriate catalytic systems. However, the control of photochemical reactions is a more difficult question since the primary intermediates involved are very short-lived excited states that may react virtually without an activation energy barrier. Classical molecular organic photochemistry studies reaction paths that, in solution, are largely determined by the functional groups in the substrate, frequently with rather modest effects of the medium. However, the interaction of the substrate with the medium constitutes one of the most powerful tools to alter its "molecular" photochemical behavior. This explains the current interest in supramolecular photochemistry, wherein the course of the irradiation is strongly influenced by the characteristics of the medium.

Among supramolecular systems to control photochemical reactions, zeolites are among the most versatile solid hosts. Although much work on organic photochemistry adsorbed in zeolites has been done by others,[1−3] this Account is limited to our Intrazeolite Photochemistry series. We include examples of the molecular control and photochemical effects that can be achieved by incorporation of an organic compound in the rigid, undeformable matrix of a zeolite of given micropore size and geometry. This Account has been organized according to the degree of molecular mobility and the type of photoprocess undergone by the guest.

Hermenegildo Garcia was born in Canals (Valencia), Spain, in 1957. He received his B.Sc. and Ph.D. degrees with Honors from the University of Valencia. He became a member of the faculty at the Polytechnical University of Valencia in 1983, where he is currently full professor. After two sabbatical leaves, joining the group of J. C. Scaiano in 1992 and 1995, he was appointed member of the Instituto de Tecnologia Quimica of Valencia. His research interests include photochemistry in solid media and heterogeneous catalysis.

J. C. (Tito) Scaiano was born in Buenos Aires, Argentina, in 1945. He studied at the Universities of Buenos Aires and of Chile and was awarded a Ph.D. degree in 1970, under the supervision of Eduardo Lissi. After a postdoctoral stay at University College London, he held positions at the University of Rio Cuarto (Argentina), the Notre Dame Radiation Laboratory, and the National Research Council of Canada. He is currently full professor at the University of Ottawa, where he studies kinetics and mechanisms of reaction intermediates in homogeneous, supramolecular, and biological systems.

Zeolites as Hosts

Zeolites are crystalline aluminosilicates[4] whose primary structure is formed by SiO_4^{4-} and AlO_4^{5-} tetrahedra sharing the edges. Their tertiary structure forms strictly uniform channels and cavities (micropores) of molecular dimensions that are repeated along the tridirectional structure of the lattice (Scheme 1). The lower valence of Al relative to that of Si creates an excess negative framework charge (one per Al) that requires charge-balancing cations to maintain electroneutrality. These associated cations are located in the interior of the pores and can be exchanged without disturbing the rigid framework.

Although some zeolites are natural minerals, most are synthesized by hydrothermal crystallization of mother gels. For some zeolites, it is possible to change moderately the framework Si/Al ratio and the charge-balancing cation during their synthesis. Zeolites can include guests in the micropores, provided they are smaller than the pore apertures. The dimensions of the pores and the geometry of the voids control the possible guest uptake and their intercavity diffusion.

Zeolites can be classified as small-, medium-, and large-pore, depending on the number of O atoms (8, 10, or 12) defining the pore apertures. Many of the limitations to incorporating large organic species inside a solid host of a narrow pore size distribution have now been overcome since novel mesoporous aluminosilicates have been reported.[5] Among them, the most widely used is MCM-41, whose internal voids are formed by parallel hexagonal channels. Even though the walls of these channels are not crystalline (in this respect, MCM-41 is not a zeolite), the remarkable channel uniformity (variable from 20 to 100 Å) and its chemical composition make MCM-41 a logical extension of the zeolite family.

Photochemistry of Large Organic Cations Incarcerated within Y Zeolite

Tridirectional zeolites encompass large cavities interconnected by smaller apertures. With this topology, it is possible for a bulky species to fit inside the cage but be too big to enter through the smaller cavity windows. In this case, we have devised "ship-in-a-bottle" syntheses, in which the final product is formed from smaller precursors. Ship-in-a-bottle strategies had been applied previously for the encapsulation of metallic complexes in zeolites.[6] We have expanded their scope to incorporate organic species, the key step being the formation of new C−C bonds rather than metal−ligand bonds (see Schemes 2−4).

Organic cations in zeolites are primarily stabilized by the polarity of the internal voids, but geometric restraints also apply when there is a tight fit of the guest inside the pores. An example of a cation with geometrical stabiliza-

† University of Ottawa.
‡ Instituto Tecnología Química.

10.1021/ar9702536 CCC: $18.00
Published on Web 08/04/1999

Scheme 1. Schematic Void Topology of Common Zeolites

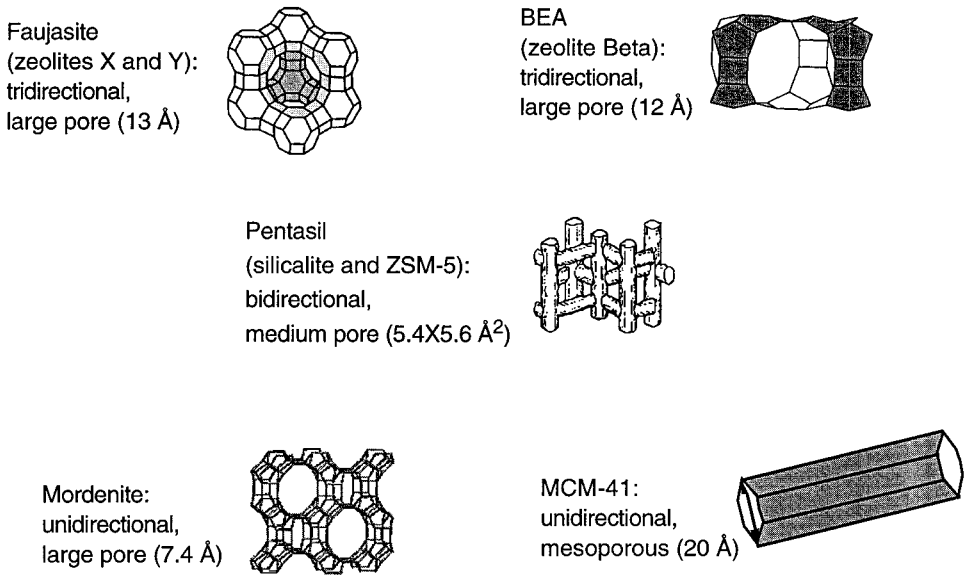

Scheme 2. Ship-in-a-Bottle Synthesis of TP^+ inside Zeolite Y

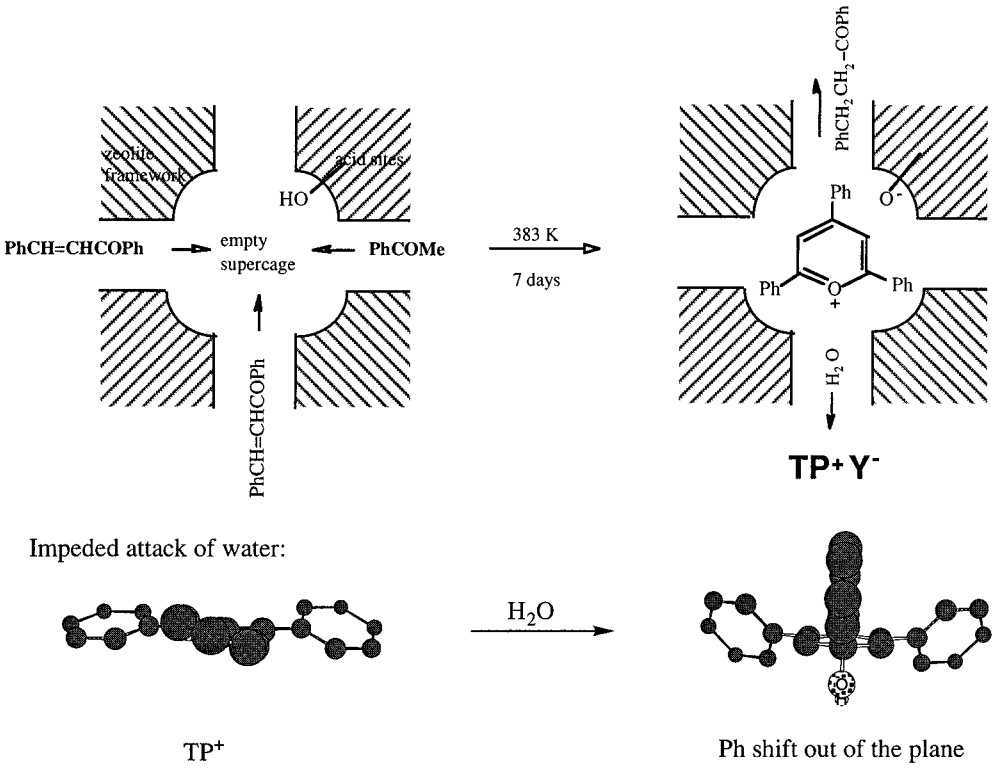

tion is 2,4,6-triphenylpyrylium ion (TP^+, Scheme 2). In water, TP^+ readily undergoes hydrolysis to form the ring-opened product, but it is completely stable when encapsulated inside Y and β zeolites.[7] Molecular modeling provides a reasonable justification for this remarkable stability. Even though H_2O can reach the TP^+ pyrylium core, its attack would require the displacement of a phenyl substituent that is impeded by the tight fit inside the cage. In contrast, simple deposition of TP^+ on the external surface of silica (no pores or cavities) does not prevent its hydrolysis.

Incorporation of TP^+ inside the zeolite supercages notably modifies many of its photophysical and photochemical properties.[8] The room-temperature emission of TP^+-Y exhibits two unresolved bands, corresponding to the simultaneous observation of fluorescence and phosphorescence (Figure 1). Coincidence of the excitation spectra with the ground-state diffuse reflectance UV−vis (DR) spectrum established that the emitting species for both bands is TP^+. It is noteworthy that TP^+ adsorbed on silica or inside mesoporous MCM-41 (30 Å diameter, loose fit) does not emit room-temperature phosphorescence.

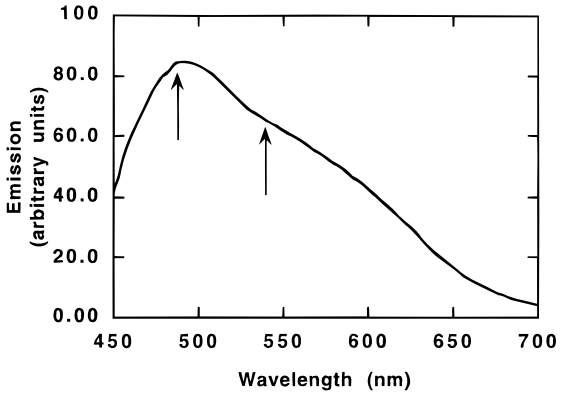

FIGURE 1. Room-temperature emission spectrum of TP^+-Y upon 420-nm excitation. The arrows indicate the fluorescence and phosphorescence maxima.

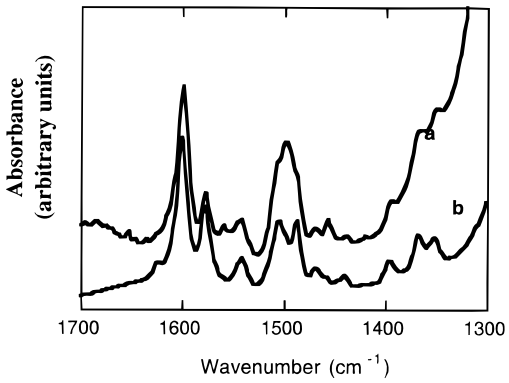

FIGURE 2. FT-IR spectra of AnX^+-HY (a) prepared by ship-in-a-bottle according Scheme 3 and AnX^+-MCM-41 (b) obtained by dehydration of AnXOH.

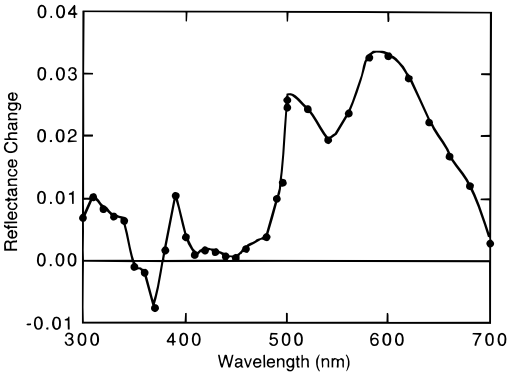

FIGURE 3. Transient DR spectrum ($\Delta J/J_0$) recorded 2 μs after 266-nm laser excitation of AnX^+-β.

This relatively high concentration of long-lived triplets upon excitation of TP^+ within Y zeolite is also related to the observation of delayed fluorescence occurring 40 ms after excitation; this does not occur in solution.[9]

The polarity of the zeolite voids and the cage effect caused by confinement are responsible for the different photochemical behavior of TP^+ embedded in zeolite or in solution.[7] Thus, laser excitation of TP^+ inside Y zeolite generates $^3TP^+$. This triplet is also detected in the laser flash photolysis (LFP) of $TP^+BF_4^-$ in aqueous acetonitrile, although a single electron transfer (ET) from H_2O to singlet or triplet TP^+ excited states is predicted to be exergonic. In contrast, the corresponding $TP^\bullet$ radical is detected in the photolysis of a slurry of TP^+-Y in water.[7] Detection of $TP^\bullet$ is indicative that ET has occurred when TP^+ is encapsulated within the Y supercages. Further, using benzene and methyl viologen as probe molecules, we have been able to obtain spectroscopic evidence for the generation of hydroxyl radicals (arising from the deprotonation of $H_2O^{+\bullet}$) by observing the formation of corresponding [arene-OH]$^\bullet$ adducts.[7]

From a preparative viewpoint, we have taken advantage of the photocatalytic ability of TP^+-Y as source of $OH^\bullet$ in the hydroxylation of benzene and the degradation of pesticides.[7,10] Remarkably, TP^+ itself is not degraded by $OH^\bullet$. Even when TP^+-Y is illuminated in distilled water for long periods, no TP^+ bleaching occurs, and a remarkable concentration of H_2O_2 (ca. 10^{-2} M) builds up. H_2O_2 is the obvious final product of coupling two $OH^\bullet$ radicals when they have no other available reaction pathways. This has led us to propose TP^+-Y as the first organic-based photocatalytic system.[7]

Another example of modification of the molecular photochemical properties of an organic cation by incarceration inside the zeolite Y supercages is the 9-(4-methoxyphenyl)xanthylium ion (AnX^+).[9] The ship-in-a-bottle synthesis of AnX^+ is shown in Scheme 3. UV−vis and IR spectra of the AnX^+-HY agree well with those of an authentic AnX^+ adsorbed in mesoporous MCM-41 (Figure 2).

The solution photochemistry of 9-arylxanthylium ions has been thoroughly studied.[11] These ions fluoresce with

Scheme 3. Synthesis of AnX^+

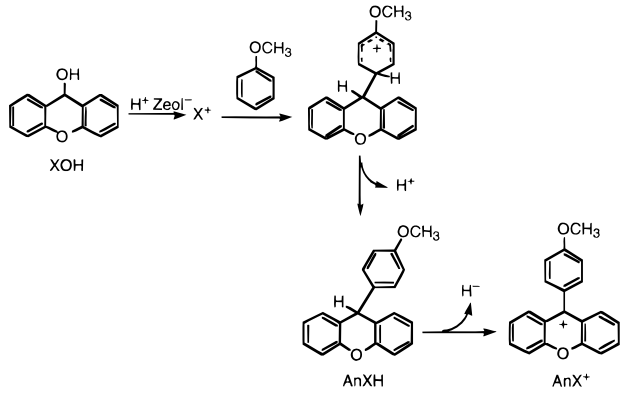

high quantum yields (Φ from 0.55 to 0.88) and have long lifetimes (1−50 ns). In addition, their triplet excited states are detectable and are characterized by an intense absorption below 300 nm and a less intense broad band in the 400−500-nm region. The only remarkable exception in this family is AnX^+, which does not fluoresce in solution at room temperature and whose triplet excited state was not detectable. These anomalies were rationalized assuming that a fast flipping of the electron-rich anisyl substituent around the electron-poor xanthyl core efficiently deactivates the first singlet excited state.

This type of radiationless deactivation requires mobility around the anisyl−xanthyl bond. According to molecular modeling, conformational freedom must be greatly re-

Scheme 4. Ship-in-a-Bottle Synthesis of T^+ inside Zeolite Supercages

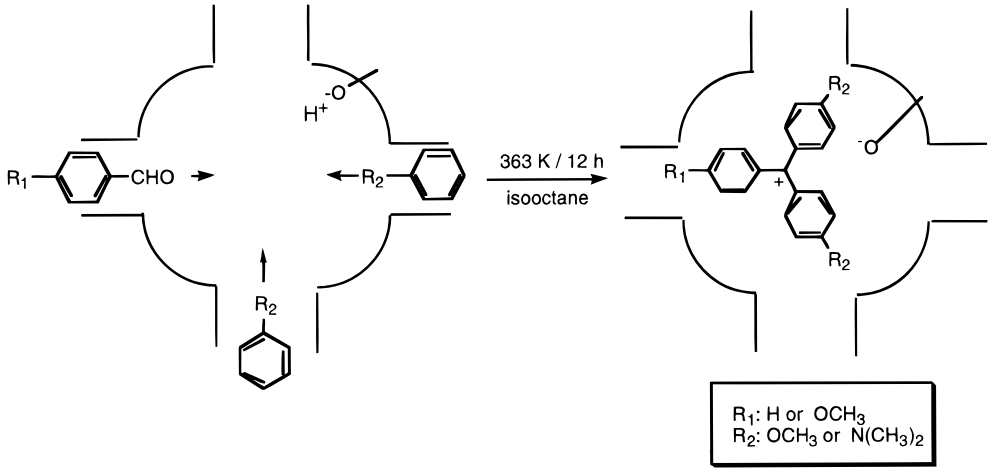

duced by incarceration of AnX^+ within the zeolite cavities. Therefore, immobilization of AnX^+ should restore its photophysical behavior to the common pattern of the 9-arylxanthyl cations. In fact, AnX^+ adsorbed in Y and β zeolites shows strong room-temperature fluorescence ($\tau \approx 4$ ns), and the triplet state is detectable by LFP (Figure 3). Furthermore, for AnX^+ adsorbed in the loose environment provided by the mesoporous MCM-41, an intermediate situation between solution and microporous zeolites was observed in terms of less intense emission, shorter singlet lifetime, and weaker 400−500-nm absorption band in the DR of $^3AnX^+$.

Analogous enhancement of fluorescence and readily detectable triplet states by restricting the conformational mobility was also found for a series of *para*-substituted trityl cations (T^+) prepared inside the zeolite Y and β supercages according to Scheme 4.[9]

For T^+ cations inside tridirectional, large-pore zeolites, the internal location inside the supercages was addressed by mapping out the C/Si atomic ratio up to ca. 30 cavities

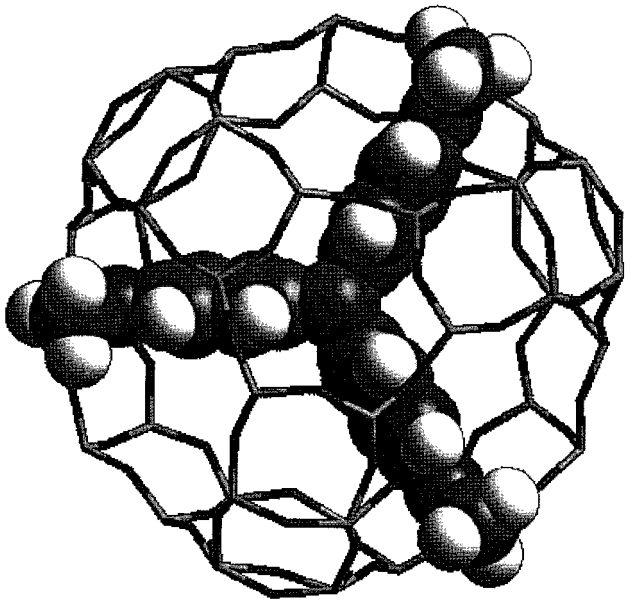

FIGURE 4. Molecular modeling of $(MeO)_3T^+$ inside the zeolite Y supercage.

Scheme 5. Rotation Leading to Optimum Conformation for $^3\beta$-PP Intramolecular Quenching

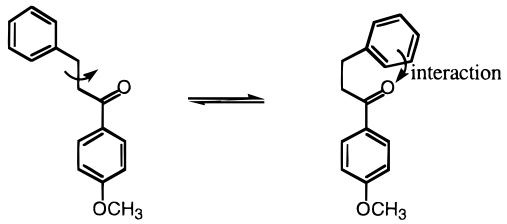

down the external surface by X-ray photoelectron spectroscopy combined with Ar^+ sputtering.[12] The C/Si ratio increases from the exterior to the interior of the particle, leveling off at about 200-Å depth. Also, high-resolution X-ray diffraction (HR-XRD) measures diffuse electron density inside the cages.[12] The Rietveldt refinement fitting of this HR-XRD gives a model (Figure 4) that agrees nicely with the best docking predicted by molecular modeling.

The consequence of the encapsulation of T^+ ions is a loss of efficiency of the nonradiative deactivation pathways and a concomitant enhancement of the emission and intersystem crossing yields.[8] For example, the normally nonfluorescent malachite green $(Me_2N)_2T^+$ emits at room temperature when adsorbed in Y zeolite, and $^3(Me_2N)_2T^+$ is readily detected by LFP.

Organic Species Rigidly Held inside Zeolite Channels

Many flexible molecules adopt a frozen stretched conformation when intubated in the channels of monodirectional zeolites that can modify their photophysical properties. A remarkable example of control of excited state reactivity is the 5 orders of magnitude increase in the triplet lifetime of β-phenylpropiophenones (β-PP) included in silicalite (a medium pore size zeolite; channels 5.75×5.15 Å^2).[13,14] In solution, β-PP does not phosphoresce due to efficient intramolecular quenching of the excited carbonyl triplet by the β-phenyl ring through a folded molecular conformation (Scheme 5). Thus, $^3\beta$-PP lifetime in toluene (ca. 1 ns) increases to 0.14 ms in silicalite. The stabilization of $^3\beta$-PP in silicalite is due to

Scheme 6. Representation of DPPs inside the Zeolite Channels

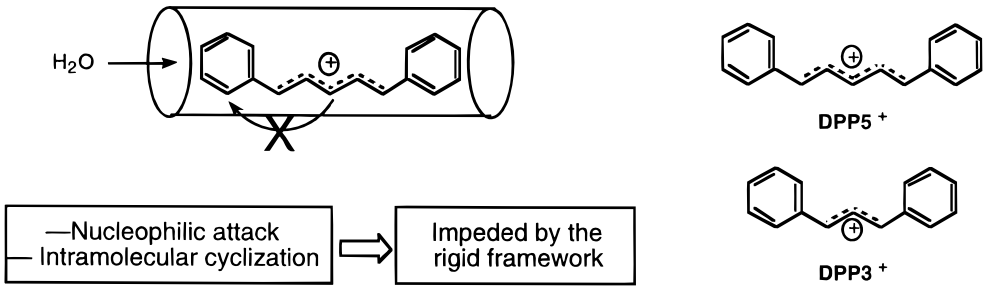

the impossibility of this molecule adopting the folded conformation required for quenching; in contrast, β-PP deposited on silica or included in mordenite (larger pore diameter) does not phosphoresce.

Just like the parent β-PP, substituted β-PP derivatives also have very short triplet lifetimes in solution.[15] This triplet lifetime is governed by how rapidly the molecule achieves the conformation suitable for intramolecular deactivation. β-PPs substituted in the *para* position by simple groups can be incorporated inside the silicalite voids, while *ortho* and *meta* derivatives are size-excluded from the pores. Only those that include well show phosphorescence.[15] Even for 4-methoxy-β-phenylpropiophenone adsorbed in the much larger cavities of NaY, a moderate increase in the triplet lifetime is observed when an "inert spectator" such as pyridine increases the geometrical congestion inside the cage, thus restricting conformational mobility.[16]

Oxygen quenching of intubated $^3\beta$-PP as well as other aromatic ketones can be interpreted by assuming the existence of *at least* two types of sites, one that is not accessible to oxygen and a second where oxygen quenching occurs efficiently and rapidly.[14] Even for the second type of sites, some kind of geometrical constraint must be experienced, since the molecules still phosphoresce.

Another example of flexible species forced to adopt a stretched conformation inside zeolite channels are the α,ω-diphenylallyl cations ($DPP3^+$ and $DPP5^+$).[17] Inclusion of DPPs leads to a major increase in their stability and persistence. Even ZSM-5 containing these allyl cations can be suspended in water for hours without disappearance of the cations. This contrasts with the reported preparation of $DPP3^+$ using FSO_3H/SO_2 in the absence of humidity. Since the parent unsubstituted allyl cation reacts and decomposes in ZSM-5, the remarkable stability of $DPP3^+$ and $DPP5^+$ inside the pores reflects the geometrical restraints imposed by the phenyl rings. We suggest that, for intubated DPPs, the phenyl caps are acting as molecular stoppers, impeding H_2O from reaching the positive (reactive) centers, and holding DPPs in an elongated conformation that prevents the intramolecular cyclization, a process that is observed in solution (Scheme 6).

The ease of generation of DPPs in zeolites makes these solids suitable for photochemical studies.[17] Thus, lamp irradiation causes isomerization around the partial C=C bonds. This was the first time that stereoisomers of allylic cations have been found to be thermally stable. Previous

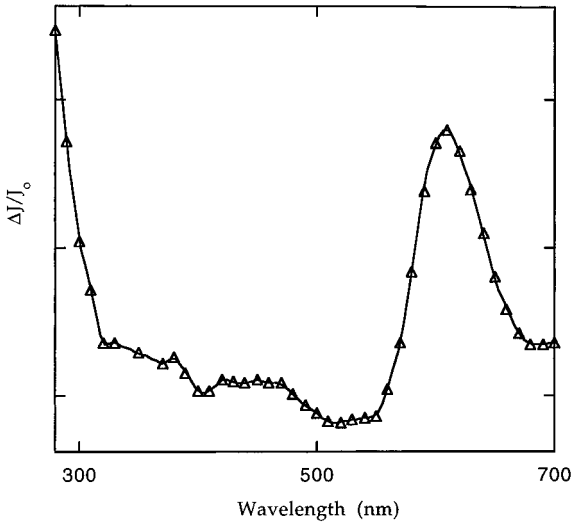

FIGURE 5. Transient DR spectrum of $DPP5^+$-ZSM-5 recorded 12 μs after 355-nm excitation.

failures to observe *cis*−*trans* isomerization in solution must be due to the need to produce them with excess acid.

The photochemical *cis*−*trans* isomerization of allyl cations within zeolites is likely to occur through the triplet excited state (not detected in solution), given that DPP triplets have been detected by LFP in zeolites as long-lived transients (ca. 100 μs) (Figure 5). Another reflection of the frozen elongated conformation of DPPs in zeolites is the observation of distinctive room-temperature emissions for the *all-E* and the *cis* stereoisomers.

Another example of an intubated guest inside zeolite channels is methyl viologen (MV^{2+}). Aqueous solutions of MV^{2+} do not fluoresce. The rotation around the bond connecting the pyridinium rings has been invoked as an efficient nonemissive deactivation pathway. In contrast, all the MV^{2+}-exchanged zeolites exhibit distinctive luminescence.[18] MV^{2+} included in zeolites of different pore sizes should experience different degrees of rotational freedom for the two heterocycles. For MV^{2+} within ZSM-5 (elliptical channels), molecular modeling predicts a frozen coplanar conformation, while the orthogonal pyridinium conformation exhibits strong unfavorable host−guest overlap. Cross-polarization magic-angle-spinning ^{13}C NMR supports the lack of conformational mobility of MV^{2+} in ZSM-5.[18] Thus, using the dipolar dephasing technique, the signals from fixed *C*−H pairs may completely decay and not be detected, while the signals from mobile *C*−H are only partially attenuated. Comparing the normal CP

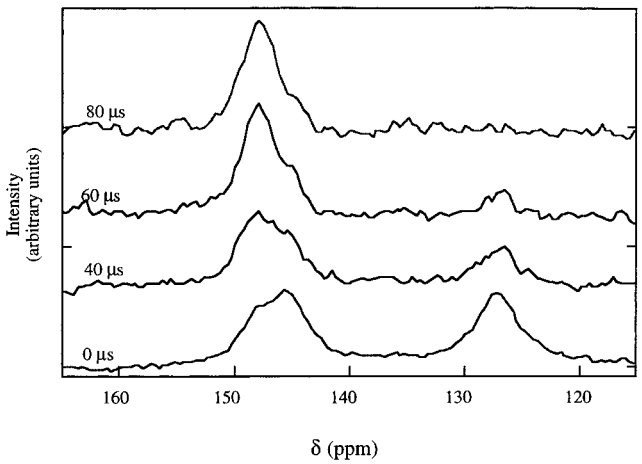

FIGURE 6. CP/MAS ^{13}C NMR of MV^{2+}-ZSM-5 at different dephasing delays.

spectrum of MV^{2+} with those recorded using dipolar dephasing, the signals of the heterocyclic C-3 completely vanished for MV^{2+} in ZSM-5 (Figure 6), while a reduction (25%) is observed in mordenite, and no noticeable differences are apparent for faujasites. In agreement with these facts, luminescence of MV^{2+}-ZSM-5 has a characteristic band at 320 nm, previously observed for MV^{2+} having a coplanar conformation (3 Å depth) in the interlamellar region of layered clays.[19] A second emission (λ_{max} = 420 nm) increases in intensity as the electron-donor ability of the zeolite framework increases and has been attributed to the emission from complexes of MV^{2+} with the framework basic sites.[18]

For less flexible species such as tricyclic xanthenium and dibenzotropylium ions[20] and neutral 1,3-diarylsquarines,[21] intubation in rigid channels causes their complete stabilization, and monodirectional zeolites are a convenient medium to study their photophysical properties (emission and detection of excited states).

Diffusion of Guests Taking Months

Pyrene has been a favorite photochemical probe for studies in many heterogeneous systems, including zeolites.[22,23] Most reports assume that the pyrene−zeolite system has reached the final stationary state shortly after sample preparation and that no further relocation−redistribution of pyrene takes place. Up to two pyrene molecules can be accommodated in a single Y supercage, but its dimensions (7.2 × 13 Å^2) are very close to the diameter of the windows of the Y supercages (7.4 Å). Even though the passage of rigid pyrene through the window is allowed, this tight fit is responsible for a remarkably slow diffusion from the outermost cavities toward the center of the particle, the relocation taking weeks. As a result, freshly prepared samples show predominant excimer emission (λ_{max} = 480 nm), with higher intensity than expected for a statistical double cage occupancy.[24] By following the evolution ("aging") of a series of pyrene−NaY samples over extended periods, an increase in monomer fluorescence at the expense of excimer emission is observed (Figure 7).[24] Eventually, in aged samples, only the monomer emission is observed. Thus, the slow intracrystalline

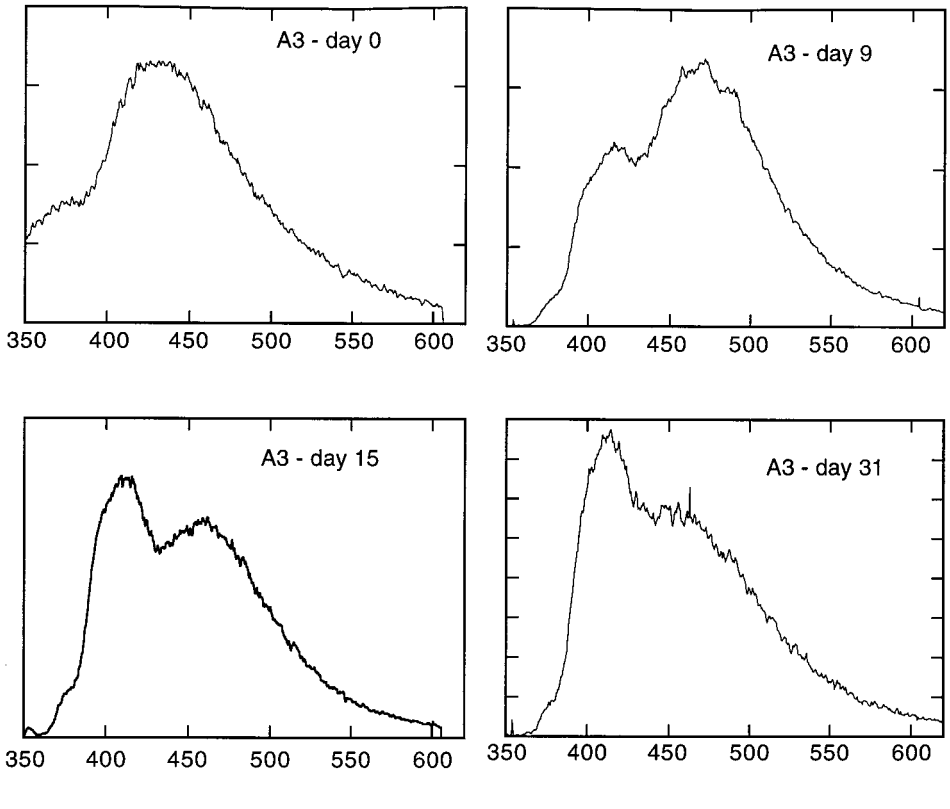

FIGURE 7. Emission spectra upon 355-nm excitation of a pyrene−NaY sample sealed under vacuum at room temperature 0, 9, 15, and 31 days after preparation.

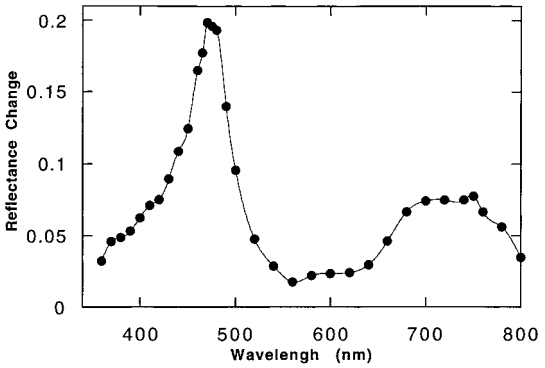

FIGURE 8. Transient DR spectrum of *trans*-stilbene included in NaX 2 μs after laser excitation.

diffusion of pyrene through the zeolite grain can be followed by recording the fluorescence over several days.

The final equilibrium distribution corresponds to isolated monomers and is the same for all pyrene samples; however, we have observed that the time required depends on the incorporation and the storage conditions.[24] Thus, vacuum-sealed samples evolve faster than those simply capped with a septum, where ambient water is slowly regained. Notably, nitrogen has a "lubricating" effect, appreciably shortening the redistribution time. An estimate based on particle size and a quadratic dependence on the number of hops and distance traveled gives about 100 s for intercavity migration. On the other hand, the 25-ps delay of the excimer emission with regard to that of monomer indicates that excimers are formed in doubly occupied cages, their formation requiring only minor reaccommodation/reorientation of two pyrenes.

Electron Exchange Processes

Electron Transfer. Molecules in zeolite cavities experience a polar environment, as indicated by molecular sensors, such as the xanthone triplet state, which undergoes extensive spectral shifts depending on environmental polarity.[25] The environment within the zeolite cavities stabilizes charged species, such as those produced in electron-transfer (ET) processes. Such processes can, in principle, involve two equal or different guests, or a guest molecule and the zeolite framework, with the latter acting as either acceptor or donor. Our work has provided examples of all of these situations.

For example, the host's role as an electron acceptor is illustrated by the photolysis of styrenes[26] and stilbenes[27] in NaX, NaY, or silicalite, wherein the corresponding radical cations have been detected by LFP (Figure 8). Laser dose dependence shows that ET is a monophotonic process.[27] For naphthalene and *p*-terphenyl, the dominant species detected are the triplet states, with radical cations being detectable but playing a secondary role.

Radical cations can also be formed by guest−guest interactions. For example, triethylamine transfers an electron to triplet acetophenone to form the corresponding radical ion pair. Now, the restricted reaction cavity favors the interaction of triethylamine radical cations with ground-state triethylamine to form amine−dimer radical cations, detected from their visible absorptions (500−600 nm).[28] This process is not observed in solution.[29] Hydrazines are formed as products of the photosensitization of acetophenone with aliphatic amines inside NaY.[28]

The zeolite framework can also act as electron donor toward a guest of appropriate oxidizing strength. Thus, $MV^{+\bullet}$ has been detected by LFP in MV^{2+}-doped zeolites.[30] The stability of $MV^{+\bullet}$ and the basic strength of alkali-exchanged Y-zeolites are directly related, with $MV^{+\bullet}$ lifetimes of several hours for RbY and CsY.

Energy Transfer. To determine the distance requirements for triplet energy transfer in NaY, we prepared a series of samples containing a constant concentration of xanthone and variable amounts of 1-methylnaphthalene.[31] Addition of 1-methylnaphthalene has two distinct effects on the triplet xanthone signals: the signal intensity (at $<$100 ns) decreases, and the decay lifetime of ^{3}xanthone changes. The first observation (*static* quenching) reflects the interaction between molecules already in close proximity at the time of excitation. This decrease in signal intensity was compared against a theoretical equation, taking into consideration the statistical distribution of 1-methylnaphthalene around xanthone molecules. This analysis led to the conclusion that energy transfer does not require xanthone and 1-methylnaphthalene to share the same supercage, but it can also occur between neighboring cavities,[31] and these processes are complete in $<$100 ns.

We and others[32] have used triplet energy transfer within zeolites in preparative photochemistry. For example, zeolite-bound organic sensitizers can be used to promote the photosensitized cyclodimerization of 1,3-cyclohexadiene (CHD), which affords two different dimer distributions, depending on whether the operating mechanism is energy or electron transfer.[33] In the first case, the [2 + 2] cycloadducts are the predominant photoproducts, while when $CHD^{+\bullet}$ is the primary intermediate, the reaction yields *exo* [4 + 2] dimer with high selectivity (Scheme 7). Heterogeneous irradiation of CHD using zeolite-bound photosensitizers can yield a dimer distribution varying from that of typical energy-transfer mechanism (4-aminobenzophenone)[33] to that characteristic of ET (TP^+ and T^+).[33]

Energy transfer in zeolites affords the opportunity for shape-selective photochemistry.[34] A remarkable example is the irradiation of *cis*- and *trans*-stilbenes in slurries of pentasil zeolites. Due to its molecular dimensions, only *trans*-stilbene can be included within the silicalite channels, while the *cis* isomer is too big to enter the pores. Thus, irradiation of a solution of *cis*-stilbene in the presence of silicalite excess leads to a photostationary state of the pure *trans* isomer. The *trans*-to-*cis* isomerization is prevented by its inclusion inside the narrow silicalite channels.[35]

The reverse isomerization (*trans* into *cis*) can also be carried out selectively by using 4-aminobenzophenone-ZSM-5 as photosensitizer.[36] Here, only the *trans*-stilbene can reach the excited 4-aminobenzophenone included

Scheme 7. Products of the Photosensitized 1,3-Cyclohexadiene Dimerization

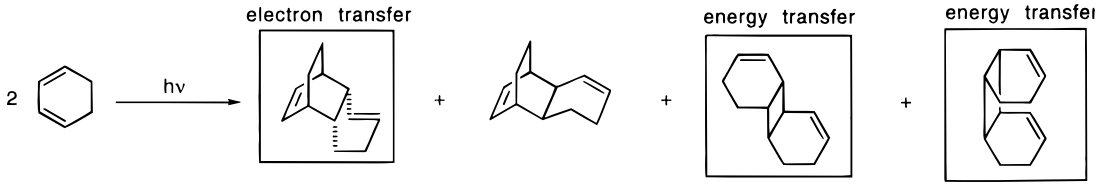

Scheme 8. Isomerization of *cis*- and *trans*-Stilbenes Using 4-Aminobenzophenone-ZSM-5 as Heterogeneous Photosensitizer

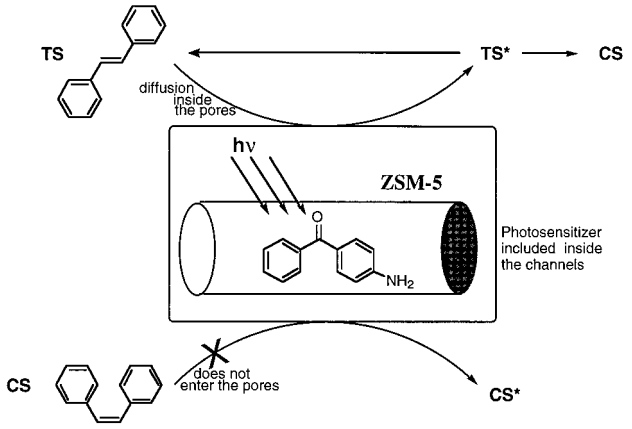

inside the channels and isomerize to *cis*-stilbene. In contrast, *cis*-stilbene does not reach the included 4-aminobenzophenone and is not photoisomerized (Scheme 8).

Acidity of Zeolites Influencing Photochemical Behavior

We already indicated that photolysis of styrenes inside NaY affords the corresponding radical cations.[26] We have observed that, during incorporation of styrenes, certain NaY samples, depending on the zeolite supplier, develop some unexpected coloration.[26] Product studies established that an acid-catalyzed dimerization has occurred. This exemplifies the influence of residual acidity in zeolites, even in their presumed neutral, Na^+ form. In the case of 4-methoxystyrene in acid zeolites, we have found that the color is due to the generation of dianisyl allyl cations (Scheme 9).[26]

This small population of acid sites in NaY can also play a role in the photochemistry of adsorbed guests. A typical example is xanthone, whose triplet excited state is readily quenched by acids. Thus, the lifetime of ^{3}xanthone in NaY is remarkably shorter than that in solution.[16] But, upon adsorption of small amounts of pyridine, the lifetime

Scheme 9. Acid-Catalyzed Dimerization of 4-Vinylanisole in Zeolites

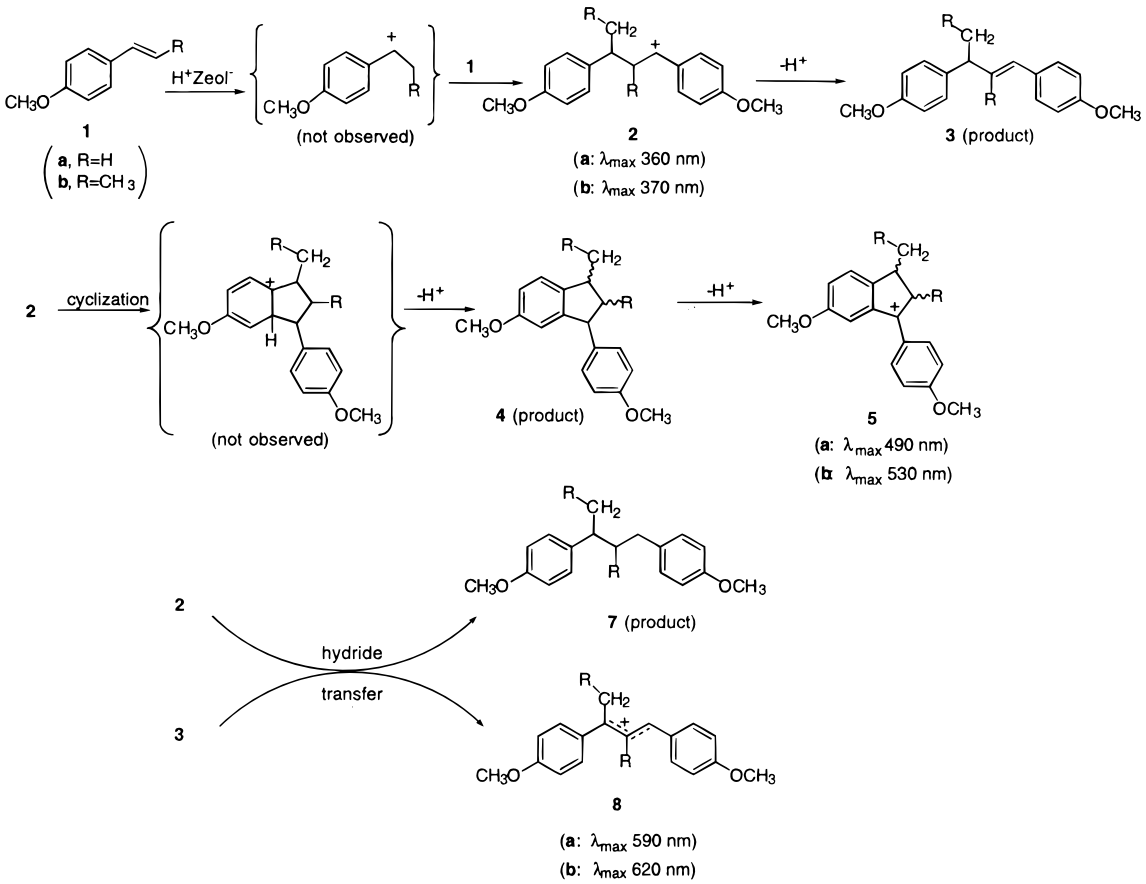

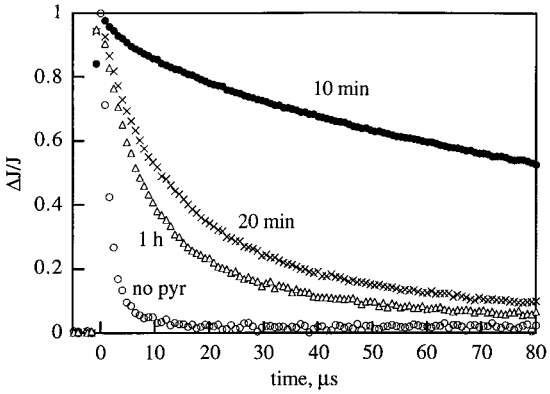

FIGURE 9. Normalized decays of triplet xanthone in NaY with different pyridine adsorption times following 355-nm excitation.

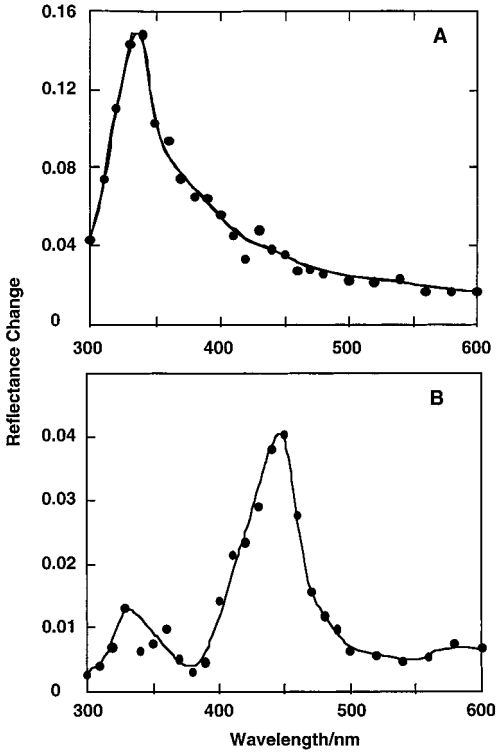

FIGURE 10. Transient DR spectra after 266-nm excitation of α,α-diphenylacetone incorporated in NaY (A, 3.2 μs after excitation) and in HYD (Si/Al 27.5) (B, 3.6 μs after excitation).

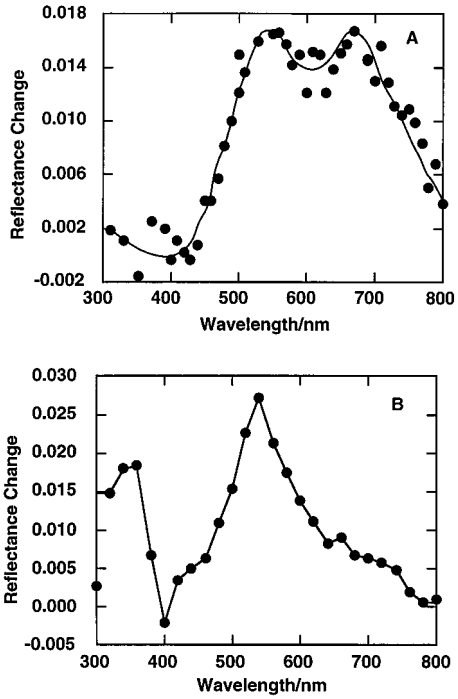

FIGURE 11. Transient DR spectra of ABP-HY (A) and ABP-HZSM-5 (B).

increases by 2 orders of magnitude (Figure 9), indicating that the small number of acid sites present in the original NaY is sufficient to quench ^{3}xanthone. Neutralization of these acid sites restores the ^{3}xanthone lifetime to the values measured in neutral solvents.

There is an increasing recognition that weak acid sites (such as those of silanols, p$K_a \approx 8$) are not inert and can participate in catalysis. To titrate these weak sites in zeolites, the standard pyridine adsorption/desorption method is inadequate. To titrate them, we have developed photochemical probes such as Coumarin-6, a fluorescent molecule that has distinctive emission spectra for the unprotonated, monoprotonated, or diprotonated form.[37]

Acidity in zeolites can play an active role in modifying the photochemistry of organic guests by protonation of their ground state. Examples are α,α-diphenyl- and 1,1,3,3-tetraphenylacetone, which upon irradiation on NaX and NaY zeolites afford diphenylmethyl radicals (DPM•), generated by homolytic cleavage. This was the first case in which time-resolved diffuse reflectance techniques were applied to detection of transient species in zeolites.[38,39] The decay kinetics of DPM• within zeolite is complex, reflecting an inhomogeneity of sites and reaction pathways,[40] but, when adsorbing the precursors in strongly acidic HY, DPM^+ rather than DPM• is detected (Figure 10).[41] The fact that α,α-diphenyl- and 1,1,3,3-tetraphenylacetone adsorbed in HY do not emit was taken as evidence that the acid sites are interacting with the carbonyl groups. The same shift from DPM• to DPM^+ as reaction intermediate is observed in the photolysis of α,α-diphenylacetone deposited on neutral clays (DPM•) or acid clays (DPM^+).[42]

The wide acid strength distribution found in the H^+ form of the zeolites and the way it can influence the photochemistry of a guest are nicely exemplified in the case of 4-aminobenzophenone.[33] The triplet excited-state spectra obtained for 4-aminobenzophenone largely depend on the acid zeolite.[33] Compared to neutral and acid solutions, the triplet spectra of 4-aminobenzophenone within zeolites range between two extreme situations, corresponding to the nonprotonated (HY) and the totally protonated 4-aminobenzophenone (HZSM-5) (Figure 11).

Concluding Remarks

Intrazeolite photochemistry has been mostly aimed at the assessment of the scope and the degree of control of the photochemical properties of adsorbed guest. Remarkable examples have already been found and the basic prin-

ciples established. Further fundamental work is needed in this area, and new examples will continue showing remarkable variations on the photochemical properties of the included guest. In this regard, we and others are using zeolites to enhance asymmetric induction in enantioselective photochemical reactions.[43,44]

The most promising future achievements can be anticipated in the application of intrazeolite photochemistry to develop chemical sensors, new photocatalytic systems, and molecular photochemical devices. Most of these applications would require the use of single large-size zeolite particles, recently developed transparent zeolite films,[45] and wafers of spatially ordered zeolite particles, but the progress in zeolite science has made these possibilities ready to be applied.

The authors acknowledge the contributions from their coworkers and colleagues. J.C.S. is generously supported by the Natural Sciences and Engineering Research Council of Canada, and H.G. by the Spanish DGICYT

References

(1) Turro, N. J.; García-Garibay, M. A. In *Photochemistry in Organized and Constrained Media*; Ramamurthy, V., Ed.; VCH: New York, 1991; pp 1−38.
(2) Ramamurthy, V. In *Photochemisty in Organized and Constrained Media*; Ramamurthy, V., Ed.; VCH: New York, 1991; Chapter 10, pp 429−493.
(3) Sun, H.; Blatter, F.; Frei, H. Selective Oxidation of Toluene to Benzaldehyde by O_2 with Visible Light in Barium^{2+} an Calcium^{2+} Exchanged Zeolite Y. *J. Am. Chem. Soc.* **1994**, *116*, 7951−7952.
(4) *Introduction to Zeolite Science and Practice*; van Bekkum, H., Flanigen, E. M., Jansen, J. C., Eds.; Elsevier: Amsterdam, 1991.
(5) Beck, J. S.; Vartuli, J. C.; Roth, W. J.; Leonowicz, M. E.; Kresge, C. T.; Schmitt, K. D.; Chu, C. T.-W.; Olson, D. H.; Sheppard, E. W.; McCullen, S. B.; Higgins, J. B.; Schlenker, J. L. A New Family of Mesoporous Molecular Sieves Prepared with Liquid Crystal Templates. *J. Am. Chem. Soc.* **1992**, *114*, 10834−10843.
(6) Balkus, K. J.; Gabrielov, A. G. Zeolite Encapsulated Metal-Complexes. *J. Inclusion Phenom. Mol. Recognit. Chem.* **1995**, *21*, 159−184.
(7) Sanjuán, A.; Alvaro, M.; Aguirre, G.; García, H.; Scaiano, J. C. Intrazeolite Photochemistry. 21. 2,4,6-Triphenylpyrylium Encapsulated inside Zeolite Y Supercages as Heterogeneous Photocatalyst for the Generation of Hydroxyl Radical. *J. Am. Chem. Soc.* **1998**, *120*, 7351−7352.
(8) Cano, M. L.; Cozens, F. L.; Fornés, V.; García, H.; Scaiano, J. C. Intrazeolite Photochemistry.12. Ship-in-a-Bottle Synthesis and Control of the Photophysical Properties of 9-(4-Methoxyphenyl)xanthenium Ion Imprisoned into Large Pore Zeolites. *J. Phys. Chem.* **1996**, *100*, 18145−18151.
(9) Cano, M. L.; Cozens, F. L.; García, H.; Martí, V.; Scaiano, J. C. Intrazeolite Photochemistry. 13. Photophysical Properties of Bulky 2,4,6-Triphenylpyrylium and Tritylium Cations within Large and Extra Large Pore Zeolites. *J. Phys. Chem.* **1996**, *100*, 18152−18157.
(10) Sanjuán, A.; Aguirre, G.; Alvaro, M.; García, H. 2,4,6-Triphenylpyrylium Ion Encapsulated in Y Zeolite as Photocatalyst: A Co-operative Contribution of the Zeolite Host to the Photodegradation of 4-Chlorophenopxyacetic Acid Using Solar Light. *Appl. Catal.: B* **1998**, *15*, 247−257.
(11) Das, P. K. Transient Carbocations and Carbanions Generated by Laser Flash Photolysis and Pulse Radiolysis. *Chem. Rev.* **1993**, *93*, 119−144.
(12) Cano, M. L.; Corma, A.; Fornés, V.; García, H.; Miranda, M.; Baerlocher, C.; Lengauer, C. Triarylmethylium Cations Encapsulated within Zeolite Supercages. *J. Am. Chem. Soc.* **1996**, *118*, 11006−11013.
(13) Casal, H. L.; Scaiano, J. C. Intrazeolite Photochemistry. I. Phosphorescence Enhancement of Aromatic Ketones Included in Silicalite. *Can. J. Chem.* **1984**, *62*, 628−629.
(14) Casal, H. L.; Scaiano, J. C. Intrazeolite Photochemistry II. Evidence for Site Inhomogneity from Studies of Aromatic Ketone Phosphorescence. *Can. J. Chem.* **1985**, *63*, 1308−1314.
(15) Scaiano, J. C.; Casal, H. L.; Netto-Ferreira, J. C. *Intrazeolite Photochemistry: Use of β-phenylpropiophenone and its Derivatives as Probes for cavity Dimensions and Mobility*; ACS Symposium Series 278; 1985; pp 211−222.
(16) Scaiano, J. C.; Kaila, M.; Corrent, S. Intrazeolite Photochemistry. 19. Effect of the "Spectator" Pyridine on the Behavior of Carbonyl Triplet States in the Zeolite NaY. *J. Phys. Chem. B* **1997**, *101*, 8564−8568.
(17) García, H.; García, S.; Pérez-Prieto, J.; Scaiano, J. C. Intrazeolite Photochemistry. 14. Photochemistry of α,ω-Diphenyl Allyl Cations within Zeolites. *J. Phys. Chem.* **1996**, *100*, 18158−18164.
(18) Alvaro, M.; Facey, G. A.; García, H.; García, S.; Scaiano, J. C. Intrazeolite Photochemistry. 16. Fluorescence of Methylviologen within Medium and Large Pore Zeolites. *J. Phys. Chem.* **1996**, *100*, 18173−18176.
(19) Villemure, G.; Detellier, C.; Szabo, A. G. Fluorescence of Clay-Intercalated Methylviologen. *J. Am. Chem. Soc.* **1986**, *108*, 4656−4659.
(20) Cozens, F. L.; García, H.; Scaiano, J. C. Intrazeolite Photochemistry. 9. Laser Flash Photolysis of Xanthenium Ion Generated by Adsorption of 9-Xanthenol within Acid Zeolites. *Langmuir* **1994**, *10*, 2246−2249.
(21) Cano, M. L.; Cozens, F. L.; Esteves, M. A.; Márquez, F.; García, H. Squaraines Inside Zeolites: Preparation, Stability and Photophysical Properties. *J. Org. Chem.* **1997**, *62*, 7121−7127.
(22) Several reports from other groups are noteworthy: Iu, K. K.; Thomas, J. K. *Langmuir* **1990**, *6*, 471. Iu, K. K.; Thomas, J. K. *J. Phys. Chem.* **1991**, *95*, 506. Suib, S. L.; Kostapapas, A. *J. Am. Chem. Soc.* **1984**, *106*, 7705. Liu, X.; Iu, K. K.; Thomas, J. K. *J. Phys. Chem.* **1989**, *93*, 4120. Liu, X.; Thomas, J. K. Study of Surface-Properties of Zeolite Faujasite Using Arenes as Photophysical Probe Molecules. *Langmuir* **1993**, *9*, 727−732. Liu, X.; Iu, K.-K.; Thomas, J. K., Photophysical Properties of Pyrene in Zeolites. Observation of Pyrene Anion Radicals in Zeolites-X and Zeolites-Y *Chem. Phys. Lett.* **1993**, *204*, 163−167. Liu, X.; Iu, K.-K.; Thomas, J. K., Photophysical Properties of Pyrene in Zeolites. A Direct Time-Resolved Diffuse-Reflectance Study of Pyrene Anio-Radicals in Zeolite-X and Zeolite-Y *J. Phys. Chem.* **1994**, *98*, 7877−7884. Liu, X.; Thomas, J. K. *Chem. Mater.* **1994**, *6*, 2303.
(23) Winnik, F. M. Photophysics of Preassociated Pyrenes in Aqueous Polymer Solutions and in Other Organized Media. *Chem. Rev.* **1993**, *93*, 587−614.

(24) Cozens, F. L.; Régimbald, M.; García, H.; Scaiano, J. C. Intrazeolite Photochemistry. 16. Influence of Aging, Inert Gases and Water on the Mobility of Pyrene Molecules on the Faujasite NaY. *J. Phys. Chem*. **1996**, *100*, 18173−18176.
(25) Scaiano, J. C. Solvent Effects in the Photochemistry of Xanthone. *J. Am. Chem. Soc.* **1980**, *102*, 7747−7753.
(26) Cozens, F. L.; Bogdanova, R.; Régimbald, M.; García, H.; Martí, V.; Scaiano, J. C. Photochemical and thermal behaviour of Styrenes within Acidic and Non-acidic Zeolites. Radical Cation versus Carbocation Formation. *J. Phys. Chem. B* **1997**, *101*, 6921−6928.
(27) Gessner, F.; Scaiano, J. C. Intrazeolite Photochemistry VII: Laser Photolysis of Stilbene and Some Aromatic Hydrocarbons in the Cavities of NaX Studies by Time-Resolved Diffuse Reflectance. *J. Photochem. Photobiol. A: Chem*. **1992**, *67*, 91−100.
(28) Scaiano, J. C.; García, S.; García, H. Intrazeolite Photochemistry. 18. Detection of Radical Cations of Amine Dimers upon Amine Photosensitization with Acetophenone in NaY. *Tetrahedron Lett.* **1997**, *38*, 5929−5932.
(29) Scaiano, J. C.; Stewart, L. C.; Livant, P.; Majors, A. M. Transient Spectroscopy and Kinetics of the Reactions of Mesocyclic Diamines with *tert*-Butoxyl and with Ketone Triplets. Effects of Ring Conformation. *Can. J. Chem*. **1984**, *62*, 1339−1343.
(30) Alvaro, M.; García, H.; García, S.; Márquez, F.; Scaiano, J. C. Intrazeolite Photochemistry 17. Zeolites as Electron Donors: Photolysis of Methyl Viologen Incorporated within Zeolites. *J. Phys. Chem*. **1997**, *101*, 3043−3051.
(31) Scaiano, J. C.; Camara de Lucas, N.; Andraos, J.; García, H. Determination of the Distance for Triplet Energy Transfer in the Faujasite NaY. *Chem. Phys. Lett.* **1995**, *233*, 5−8.
(32) Pitchumani, K.; Gamlin, J. N.; Ramamurthy, V.; Scheffer, J. R. Triplet−triplet Energy Transfer Between Organic Molecules Trapped in Zeolites. *Chem. Commun*. **1996**, 2049−2050.
(33) Baldoví, M. V.; Cozens, F. L.; Fornés, V.; García, H.; Scaiano, J. C. Intrazeolite Photochemistry. 11. Modification of the Properties of the Energy Transfer Photosensitizer 4-Aminobenzophenone by Immobilization within Different Zeolite Microenvironments. *Chem. Mater.* **1996**, *8*, 152−160.
(34) Turro, N. J.; Cheng, C.-C.; L., A.; Corbin, D. R. Size, Shape, and Site Selectivities in the Photochemical Reactions of Molecules Adsorbed on Pentasil Zeolites. Effects of Coadsorbed Water. *J. Am. Chem. Soc.* **1987**, *109*, 2449−2456.
(35) Gessner, F.; Olea, A.; Lobaugh, J. H.; Johnston, L. J.; Scaiano, J. C. Intrazeolite Photochemistry. 5. Use of zeolites in the Control of Photostationary Ratios in Sensitized Cis−Trans Isomerizations. *J. Org. Chem*. **1989**, *54*, 259−261.
(36) Baldoví, M. V.; Corma, A.; García, H.; Martí, V. Shape-selective Photosensitized Isomerization of Stilbene Using a Benzophenone Incorporated Within Acid Zeolites. *Tetrahedron Lett.* **1994**, *35*, 9447−9450.
(37) Corrent, S.; Hahn, P.; Pohlers, G.; Connolly, T.; Scaiano, J. C.; Fornés, V.; García, H. Intrazeolite Photochemistry. 22. Acid Base Properties of Coumarin 6. Characterization in Solution, the Solid State and Incorporated into Supramolecular Systems. *J. Phys. Chem*. **1998**, *102*, 5852−5858.
(38) Kelly, G.; Willsher, C. J.; Wilkinson, F.; Netto-Ferreira, J. C.; Olea, A.; Weir, D.; Johnston, L. J.; Scaiano, J. C. Intrazeolite Photochemistry. VI. Diffuse Reflectance Laser Flash Photolysis and Product Studies of Diphenylmethyl Radicals on Solid Supports. *Can. J. Chem*. **1990**, *68*, 812−819.
(39) Bohne, C.; Redmond, R. W.; Scaiano, J. C. In *Photochemistry in Organized and Constrained Media*; Ramamurthy, V., Ed.; VCH: New York, 1991; Chapter 3, pp 79−132.
(40) Johnston, L. J.; Scaiano, J. C.; Shi, J.-L.; Siebrand, W.; Zerbetto, F. Observation and Modelling of the Recombination Kinetics of Diphenylmethyl Radicals in the Cavities of Na-X Zeolite. *J. Phys. Chem*. **1991**, *95*, 10018−10024.
(41) Cozens, F. L.; García, H.; Scaiano, J. C. Intrazeolite Photochemistry. 8. Influence of the Zeolite Physicochemical Parameters on the Laser Flash Photolysis of 1,1-Diphenyl-2-propanone Included in Acid Faujasites. *J. Am. Chem. Soc.* **1993**, *115*, 11134−11140.
(42) Cozens, F. L.; García, H.; Gessner, F.; Scaiano, J. C. Cooperative Effect of Surface Sites on the Laser Flash Photolysis of 1,1-Diphenylacetone and 1,1,3,3-Tetraphenylacetone Adsorbed on Layered Clays. Generation of Radicals and Carbocations. *J. Phys. Chem*. **1994**, *98*, 8494−8497.
(43) Sundarababu, G.; Leitbovitch, M.; Corbin, D. R.; Scheffer, J. R.; Ramamurthy, V. Zeolite as a Host for Chiral Induction. *Chem. Commun.* **1996**, 2159−2160.
(44) Sabater, M. J.; García, S.; Alvaro, M.; García, H.; Scaiano, J. C. Intrazeolite Photochemistry. 24. Enantioselective Discrimination in the Quenching of Chiral Mn(II)salen Complexes Encapsulated inside Y Zeolite by Chiral 2-Butanols. *J. Am. Chem. Soc.* **1998**, *120*, 8521−8522.
(45) Alvaro, M.; García, H.; Corrent, S.; Scaiano, J. C. Intrazeolite Photochemistry. 23. Transparent PDMS Films of Zeolites Incorporating Organic Guests: Quantitative Determination of Photophysical Parameters by Transmission Techniques. *J. Phys. Chem*. **1998**, *102*, 7530−7534.

AR9702536